Ascorbic Acid Free Radicals. I. Pulse Radiolysis Study of Optical Absorption and Kinetic Properties[1]

Benon H. J. Bielski,* David A. Comstock, and Richard A. Bowen

Contribution from the Chemistry Department, Brookhaven National Laboratory, Upton, New York 11973.
Received February 24, 1971

Abstract: Absorption spectra of L-ascorbic acid free radicals generated in aqueous solutions (pH −0.3 to 11) by pulse radiolysis were determined. Variation in extinction coefficients with pH suggests that the radicals can exist in a protonated form ($AH_2\cdot^+$), as a neutral species ($AH\cdot$), and as anion radicals ($A\cdot^-$), with pK values of 1.10 and 4.25. The radicals decayed by second-order kinetics throughout the entire pH range. A mechanism is proposed which accounts for the observed acid-catalyzed decay. Ionic strength effects at various pH's are consistent with charges assigned to the various radical species.

It is well known that the oxidation of ascorbic acid (AH_2) to dehydroascorbic acid (A) is a reversible process, which proceeds in two steps with the formation of a free radical ($AH\cdot$) as an intermediate. Since from the biological viewpoint the redox reaction is the most outstanding chemical characteristic of ascorbic acid, the importance of the free radical needs little comment.

First successful studies of the radical were reported by Yamazaki, *et al.*[2-4] They proved the existence of the free radical *in vitro* by electron spin resonance and showed that it decays by second-order kinetics. Duke,[5] using the same technique, demonstrated that the radical can also be observed *in vivo*. While Yamazaki, *et al.*,[3] and Lagercrantz[6] postulated that the radical is formed by removal of an electron from the HO group on C_2, Förster, *et al.*,[7] and Kluge, *et al.*,[8] produced fairly convincing evidence that the primary oxidative attack on ascorbic acid takes place at the HO group of C_3.

The feasibility of studying the ascorbic acid radical by pulse radiolysis was suggested by the work of Barr and King.[9] In the report on the effect of ^{60}Co γ rays upon aqueous ascorbic acid solutions, the authors postulated the formation of the radical ($AH\cdot$) as the first product of OH and HO_2 radical attack upon the parent compound (AH_2). This supposition was supported by subsequent studies of Rao[10] and Ogura, *et al.*[11] Conclusive evidence for generation of the ascorbic acid radical by ionizing radiation was found by Bielski and Allen,[12] who recorded its optical absorption spectrum. Their spectrophotometric decay measurements of the radical are in close agreement with values determined for enzymatic oxidation by Yamazaki.[3]

This report is a continuation and extension of the earlier work.

Experimental Section

Chemicals. L-Ascorbic acid, reagent grade (Fisher Scientific Co.), was used without further purification. L-Ascorbic-*1*-^{14}C acid (International Chemical and Nuclear Corp.) was further purified by chromatography.[13] Dehydroascorbic acid (Nutritional Biochemical Corp.) was purified by the method of Staudinger and Weiss.[14]

Solutions. All solutions were prepared in triply distilled water. The sodium hydroxide solutions were free of CO_2. Perchloric acid was purified before use by distillation over a 40-plate column. Phosphate solutions were prepared from reagent grade chemicals without further purification.

Apparatus. The electron pulse generators (2-MeV Van de Graaff and Febetron), optics, and monitoring equipment have been described in an earlier publication.[15,16] The optical path length was 6.2 cm.

Results

Ascorbic acid free radicals can be generated during radiolysis of aqueous solutions by oxidation of ascorbic acid by hydroxyl radicals (2), by reduction of dehydroascorbic acid by hydrated electrons (3), or by atomic hydrogen (4) ($AH\cdot$ represents the radical without regard to its state of ionization).

$$H_2O \rightsquigarrow H,\ e_{aq}^-,\ OH,\ H_2O_2,\ H_2 \qquad (1)$$

$$AH_2 + OH \longrightarrow AH\cdot + H_2O \qquad (2)$$

$$A + e_{aq}^- \xrightarrow{H^+} AH\cdot \qquad (3)$$

$$A + H \longrightarrow AH\cdot \qquad (4)$$

Since the oxidative and reductive species are formed in almost equal amounts during radiolysis of water,[17-19] two experimental conditions were chosen so that only one type of radical $AH\cdot$ is generated quantitatively. In general, $G(AH\cdot) = G_{e_{aq}^-} + G_H + G_{OH}$, where G repre-

(1) Research performed under the auspices of the U. S. Atomic Energy Commission.
(2) I. Yamazaki, H. S. Mason, and L. Piette, *Biochem. Biophys. Res. Commun.*, 1, 336 (1959).
(3) I. Yamazaki, H. S. Mason, and L. Piette, *J. Biol. Chem.*, **235**, 2444 (1960).
(4) I. Yamazaki and L. H. Piette, *Biochim. Biophys. Acta*, **50**, 62 (1961).
(5) P. S. Duke, *Exp. Mol. Pathol.*, **8**, 112 (1968).
(6) C. Lagercrantz, *Acta Chem. Scand.*, **18**, 562 (1965).
(7) G. V. Förster, W. Weis, and H. Staudinger, *Justus Liebigs Ann. Chem.*, **690**, 166 (1965).
(8) H. Kluge, R. Rasch, B. Brux, and H. Frunder, *Biochim. Biophys. Acta*, 141, 260 (1967).
(9) N. F. Barr and C. G. King, *J. Amer. Chem. Soc.*, **78**, 303 (1956).
(10) B. S. N. Rao, *Radiat. Res.*, **5**, 683 (1962).
(11) H. Ogura, M. Murata, and M. Kondo, *Radioisotopes*, **19**, 89 (1970).
(12) B. H. J. Bielski and A. O. Allen, *J. Amer. Chem. Soc.*, **92**, 3793 (1970).
(13) I. M. Hais and K. Macek, "Paper Chromatography," Academic Press, New York, N. Y., 1963, p 679.
(14) H. Staudinger and W. Weiss, *Z. Physiol. Chem.*, **337**, 284 (1964).
(15) B. H. J. Bielski and H. A. Schwarz, *J. Phys. Chem.*, **72**, 3836 (1968).
(16) I. G. Draganić, Z. D. Draganić, and R. A. Holroyd, *ibid.*, in press.
(17) A. O. Allen, "The Radiation Chemistry of Water and Aqueous Solutions," Van Nostrand, Princeton, N. J., 1961.
(18) B. H. J. Bielski and A. O. Allen, *Int. J. Radiat. Phys. Chem.*, 1, 153 (1969).
(19) J. H. O'Donnell and D. F. Sangster, "Principles of Radiation Chemistry," American Elsevier, New York, N. Y., 1970.

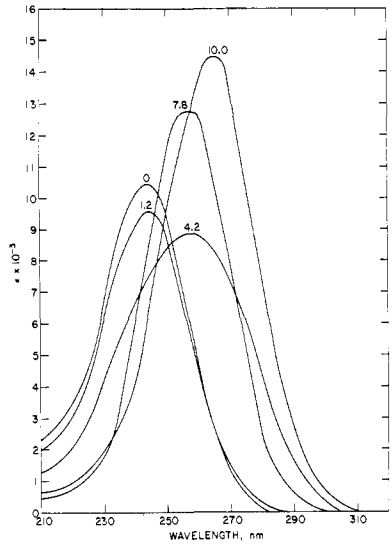

Figure 1. Absorption spectra of ascorbic acid at 23.5°. At pH 0.0 and 1.2, measurements were taken in $HClO_4$ solutions. pH 4.2, 7.8, and 10.0 were adjusted by addition of NaOH.

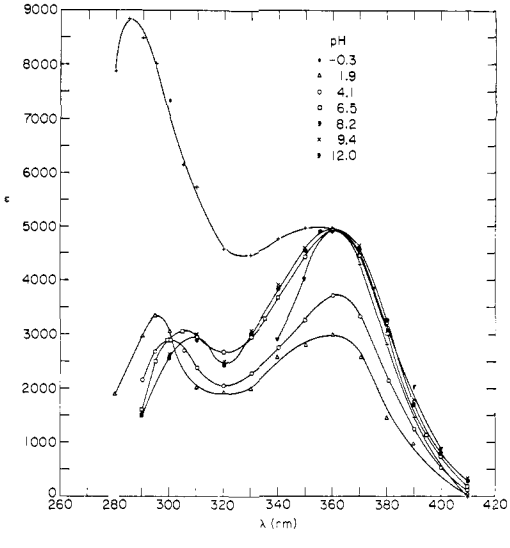

Figure 2. Absorption spectra of ascorbic acid free radicals. The spectra at pH −0.3 and 1.9 were determined in $HClO_4$ solutions. The spectrum at 4.1 was determined in an ascorbic acid solution to which sodium hydroxide had been added. The spectra at pH 6.5, 8.2, 9.4, and 12 were determined in 0.05 *M* phosphate buffer.

sents the number of molecules formed per 100 eV of energy absorbed.

System A was an equimolar solution (1–5 m*M*) of ascorbic and dehydroascorbic acids saturated with argon. This was used in the pH range between −0.3 and 3.9. The acidity of these solutions was adjusted by addition of $HClO_4$, H_2SO_4, or NaOH. Formation of AH· in this system is described by reactions 2, 3, and 4. The yield is assumed to be $G(AH\cdot) = 6.1$ radicals/100 eV.

System B refers to ascorbic acid solutions (1–5 m*M*) saturated with nitrous oxide used above pH 3.5. The pH of these solutions was adjusted by addition of NaOH or phosphate buffers. Under these conditions the nitrous oxide reacted rapidly with the hydrated electron (5) to yield hydroxyl radicals[20] which were

$$N_2O + e_{aq}^- + H_2O \longrightarrow N_2 + OH + OH^- \qquad (5)$$

scavenged by ascorbic acid (2) to yield AH·. Since the yield of OH radicals generated in a N_2O-saturated solution is 6.45 radicals/100 eV, it was assumed that this value also represents the total number of AH· radicals formed. The observed yields of AH· were consistent between the two systems at pH 3.9.

Product Analysis. Two samples of a 5 m*M* ascorbic acid solution (pH 3.2) containing L-ascorbic-*1*-^{14}C acid (specific activity 1.2 mCi/mmol) were saturated with N_2O and irradiated with 10-μsec electron pulses. One sample received 1600 rads and the other 4000 rads per pulse. The products, along with control blanks, were chromatographed (descendent, argon atmosphere, *n*-BuOH, AcOH, H_2O) on Whatman No. 1 paper.

The chromatogram was subsequently analyzed by contact with an X-ray plate (Cronex 4, Du Pont) for 5 days. The developed plate was examined for number of components and R_f values. The same chromatogram was also analyzed on a Varian radioscanner. The results showed only two spots, one representing ascorbic acid ($R_f = 0.37$) and the other dehydroascorbic acid ($R_f = 0.48$). Since this method is very sensitive, it appeared that only dehydroascorbic acid was formed from ascorbic acid under the conditions employed.

Absorption Spectra. Absorption spectra of ascorbic acid (Figure 1) were determined on a Cary 14 spectrophotometer at 23.5°. The pH of solutions was adjusted by the addition of either sodium hydroxide or perchloric acid. To prevent air oxidation, all solutions were purged with argon.

The spectra of ascorbic acid free radicals are given in Figure 2. They represent the molar absorbance as a function of wavelength at the end of a 30-μsec pulse. The individual experimental points were obtained by extrapolation of second-order decay plots to the end of the pulse. The energy input per pulse was kept constant (150–200 rads) during the determination of a particular spectrum. After appropriate corrections for energy input deviations (of the order of 4–6%), the spectrum was normalized in terms of the extinction coefficient determined at 360 nm (see below).

The spectra show two distinct maxima, one in the wavelength region 285–310 nm, and the other at 360 nm. The shorter wavelength absorption is subject to a red shift with decreasing acidity. Actually, the spectra represent $\epsilon_{AH\cdot} - \epsilon_{AH_2}$, since one ascorbic acid is destroyed for each AH· formed. The red shift probably represents the red shift of the ascorbic acid spectrum with pH (see Figure 1).

Molar extinction coefficients of AH· determined at 360 nm (23.5°) as a function of pH are shown in Figure 3. The numerical values of ϵ were computed from the plateau regions of $(OD)_0$/(energy per pulse) *vs.* (energy per pulse) graphs (see Figure 4), where $(OD)_0$ represents the optical absorbance at the end of a 10-μsec pulse. Consistent results were obtained for energy inputs of up to 200 rads per pulse. Above this energy the slope decreased, probably because of interaction of ascorbic acid radicals with OH during the pulse.

$$AH\cdot + OH \longrightarrow A + H_2O \qquad (6)$$

This assumption is supported by product analysis and

(20) M. Anbar and P. Neta, *Int. J. Radiat. Isotopes*, 16, 229 (1965).

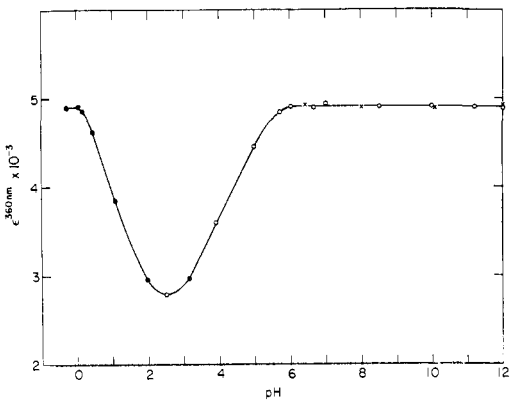

Figure 3. Molar extinction coefficients of ascorbic acid radicals at 360 nm (23.5°) as a function of pH: ●, $HClO_4$ solutions; ◐, natural pH 3.16; ○, pH 3.9–12, NaOH added; ×, 0.02 *M* phosphate.

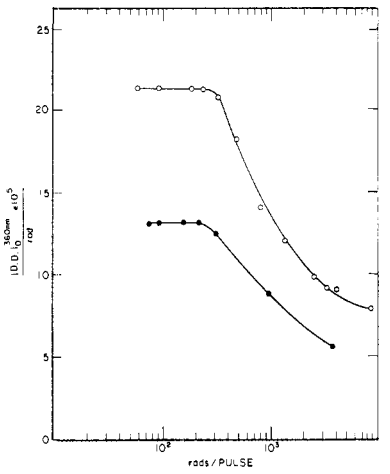

Figure 4. Optical absorbance per unit absorbed energy (6.2-cm light path, 360 nm) at the end of a 10-μsec pulse, in 1 m*M* AH_2 as a function of energy input per pulse: ●, pH 3.16 (system A); ○, pH 5.76 (system B, 0.02 *M* phosphate).

consistent second-order decay over a wide range of energy input per pulse (Figure 5).

The molar extinction coefficients given in Figure 3 were independent of ascorbic acid concentration (10^{-4}–10^{-2} *M*), $HClO_4$, H_2SO_4, and NaOH over the pH range studied (−0.3 to 12). In contrast, addition of phosphate buffer did affect the extinction coefficients below pH 5.1 as shown by the values listed at pH 3.61 in Table I. At pH 5.1 and above, addition of phosphate up to 0.1 *M* did not affect the extinction coefficients measured at 360 nm.

Table I. Molar Extinction Coefficient of AH· Radicals in the Presence of Phosphate[a]

ε (360 nm)	Phosphate, *M*
3340	0.000
2780	0.010
2290	0.025
1950	0.050
1730	0.100

[a] System B, 1 m*M* AH_2; 10-μsec pulse, pH 3.61 (H_3PO_4 + NaOH), temperature 23.5°.

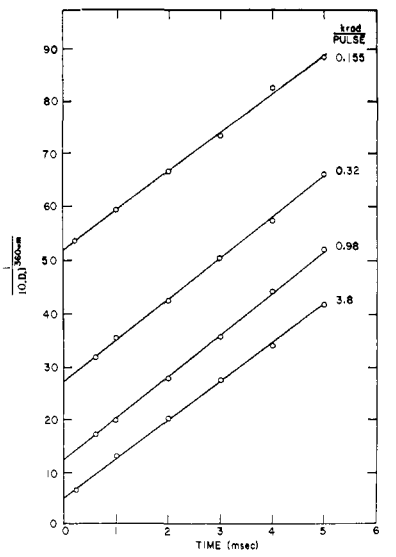

Figure 5. Second-order decay of ascorbic acid radicals at 23.5°, pH 3.16. The radicals were generated by 10-μsec pulses of increasing energy in system B. Optical light path, 6.2 cm.

Preliminary studies indicated at pH 4 that the two absorption maxima of ascorbic acid free radicals can be assigned to the following tautomeric forms.

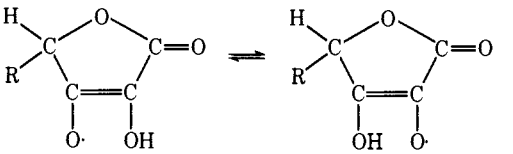

maximum at 360 nm maximum at 290 nm

This assumption is based on observed radical spectra of 3-methylascorbic acid, 1-methylascorbic acid, and 2,3-dimethylascorbic acid, which have single maxima at 290, 390, and 330 nm, respectively. Conclusive assignment will be possible after determination of the 2-methylascorbic acid radical spectrum.

It was also observed that the molar extinction coefficients of ascorbic acid radicals undergo small changes with temperature. Since these changes have to be determined at all pH values of interest, the thermodynamic properties of the radicals will be published upon completion of these experiments.

Rate of Radical Decay. The rate of formation of the ascorbic acid free radical in reaction 2 is fast compared to its decay under present experimental conditions. Adams[21] reported a rate constant for (2) at pH 1, $k = 7.2 \times 10^9\ M^{-1}\ \text{sec}^{-1}$.

Product analysis and decay kinetics of the ascorbic acid free radical suggest a disproportionation mechanism described by the following equations.

$$\text{AH}\cdot + \text{AH}\cdot \xrightarrow{k_{obsd}} \text{A} + \text{AH}_2 \qquad (7)$$

$$-\text{d(AH}\cdot)/\text{d}t = 2k_{obsd}(\text{AH}\cdot)^2 \qquad (I)$$

The rate constant k_{obsd} was determined following 30-μsec pulses with an average input of 600–800 rads per pulse at 360 nm. The pH of these solutions was ad-

(21) G. E. Adams, J. W. Boag, J. Currant, and B. D. Michael, "Pulse Radiolysis," Proceedings of the International Symposium held at Manchester, England, April 1965, Academic Press, New York, N. Y., 1965, p 137.

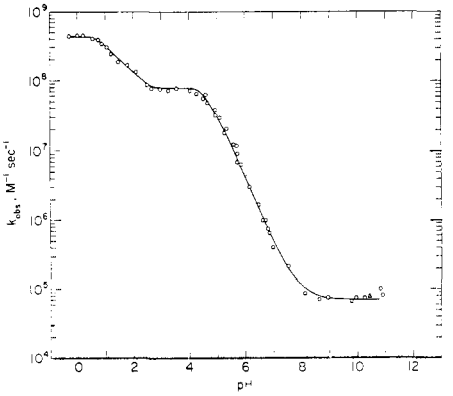

Figure 6. Second-order decay constants, k_{obsd}, for ascorbic acid radicals as a function of pH, which was adjusted by addition of $HClO_4$, H_2SO_4, and NaOH: O, experimental rate constants; —, curve computed from eq II.

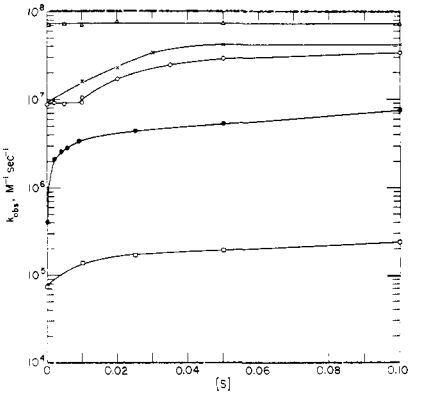

Figure 7. Change in k_{obsd} with solute concentration [S] (system B conditions): Δ, ascorbic acid (variable) from 1 mM (natural pH 3.6) to 100 mM (natural pH 2.6); O, ascorbic acid (variable) adjusted to pH 5.76 with NaOH; ×, 1 mM ascorbic acid in phosphate buffer (variable) pH 5.76; ●, 1 mM ascorbic acid in phosphate buffer (variable) pH 6.91; □, 1 mM ascorbic acid in phosphate buffer (variable) pH 8.67.

justed by addition of $HClO_4$, H_2SO_4, and NaOH only. The results are shown in Figure 6.

To study the second-order decay kinetics, the initial concentration of the radicals was varied by changing the energy input per pulse. Solutions of 1 mM ascorbic acid were irradiated at pH 3.16 (system A) over a 24.5-fold energy range (Figure 5) and at pH 6.91 (system B) over a 10-fold energy range (Table II). The kinetics

Table II. Second-Order Rate Constant as a Function of Pulse Energy[a]

Rads/pulse	k_{obsd}, M^{-1} sec^{-1}
180	4.53×10^5
374	4.93×10^5
632	5.09×10^5
1800	4.90×10^5

[a] System B, 1 mM AH_2^-; 10-μsec pulse; pH 6.91 (NaOH added), temperature 23.5°.

and k_{obsd} remained unchanged.

Experiments carried out at pH 6.91 in the absence of buffer served still another purpose. The removal of increasing quantities of AH^- in reaction 8 by raising the

$$AH^- + OH \longrightarrow A\cdot^- + H_2O \qquad (8)$$

energy per pulse shifts the ascorbic acid dissociation equilibrium. This causes a shift in pH which should lead to a drop in k_{obsd}, especially near neutrality, where k_{obsd} varies rapidly with pH (Figure 6). However, no such change was observed (Table II). The most probable explanation for this lies in the similarity of the AH· and AH_2 pK values (see the Discussion section) which causes the system to be effectively buffered internally.

A single experiment with D-ascorbic acid indicated that the decay of its radical at pH 3.2 is the same as that of the L form, assuming their extinction coefficients to be identical.

Effect of Solute Concentration upon k_{obsd}. Rate constant measurements (600 rads/10-μsec pulse) were carried out in ascorbic acid solutions which varied in concentrations from 1 mM (natural pH 3.6) to 100 mM (natural pH 2.6). These variations had no effect upon the decay rate of the radical (Figure 7). When the solutions were adjusted to pH 5.76 by addition of sodium hydroxide, k_{obsd} was constant only up to 10 mM ascorbate (AH^-). At higher concentrations the rate increased, as shown in Figure 7.

Addition of phosphate buffer to ascorbic acid solutions (system B, 1 mM AH_2) also produced a marked increase in k_{obsd}. The increase was observed at all pH values studied (Figure 7 and Table III). Results in Table III are given in terms of k/ϵ, since below 5.1 the

Table III. Effect of Phosphate Concentration upon k_{obsd}/ϵ as a Function of pH[a]

pH	k_{obsd}/ϵ in 0.02 M phosphate	pH	k_{obsd} in 0.10 M phosphate
2.30	3.16×10^4	4.0	2.85×10^4
3.56	2.65×10^4	4.96	2.15×10^4
4.05	2.50×10^4	5.78	9.40×10^3
4.70	1.65×10^4	6.90	1.65×10^3
5.40	1.05×10^4	7.97	1.85×10^2
5.87	4.30×10^3	8.54	8.40×10^1
6.46	1.45×10^3	9.14	4.20×10^1
7.13	3.85×10^2	9.63	5.20×10^1
7.59	1.95×10^2	10.13	6.95×10^1
8.14	5.20×10^1	10.79	1.32×10^2
8.65	3.30×10^1		
9.08	1.80×10^1		
9.96	1.61×10^1		
10.46	1.77×10^1		

[a] System B, 1 mM AH_2^-; 600 rads/10-μsec pulse, 23.5°.

molar extinction coefficient of the radical varies with phosphate concentration. It is apparent that this increase was most pronounced near neutrality and in the low phosphate concentration region. To establish if the change was dose-rate dependent, 0.01 M phosphate solutions (system B, 1 mM AH_2^-, pH 6.91) were irradiated with 10-μsec pulses of up to 3.4 krads. Neither k_{obsd} nor the order of decay was affected (Table IV).

The ionic strength effect was studied at pH 3.3 and 9.8 using sodium perchlorate to vary μ. Ascorbic acid concentration was kept at 1 mM. The pH was adjusted with sodium hydroxide or perchloric acid. In all cases the amount of acid or base added was insufficient to change μ. As shown in Figure 8, at pH 3.3 there was no effect, but at pH 9.8 there was a pronounced increase in the rate constant with increase in μ.

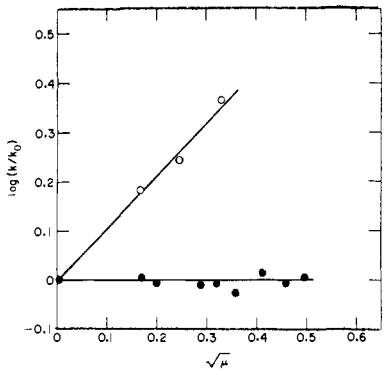

Figure 8. Effect of ionic strength upon the rate of decay of ascorbic acid radicals at pH 3.3 (○) and 9.8 (●).

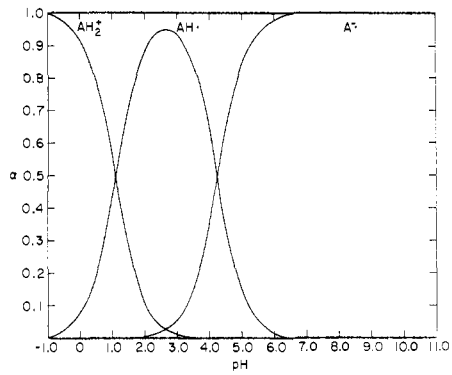

Figure 9. Per cent fraction (α) as a function of pH.

Discussion

Changes in the molar extinction coefficient at 360 nm with pH (Figure 3) suggest that the ascorbic acid radical can exist in a protonated form ($AH_2^+\cdot$), as a neutral species ($AH\cdot$), and in an ionized form ($A\cdot^-$)

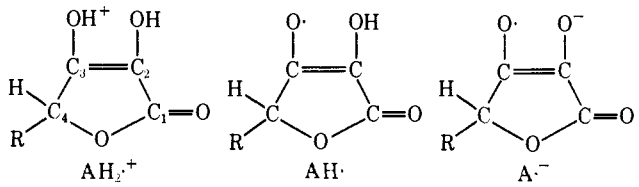

where R = $CHOHCH_2OH$. AH_2^+ and A^- have resonance forms with the charge on C_2 and C_3, of course, analogous to the two tautomeric forms of $AH\cdot$.

Table IV. Effect of Pulse Strength on Rate of Decay[a]

krads/pulse	k_{obsd}, M^{-1} sec^{-1}
0.244	3.62×10^6
0.474	3.55×10^6
0.599	3.72×10^6
0.610	3.63×10^6
1.497	3.45×10^6
3.382	3.63×10^6

[a] System B, 0.01 M phosphate, 10-μsec pulse, pH 6.91.

Since measurements at both absorption maxima gave identical decay rates at pH 3.16, 5.78, 6.48, and 8.20, we can assume that rapid equilibrium exists between the different radical species at a given pH. The corresponding pK values computed from Figure 3 are

$$AH_2\cdot^+ \underset{}{\overset{pK_1 = 1.10}{\rightleftharpoons}} AH\cdot + H^+ \quad (9)$$

$$AH\cdot \overset{pK_2 = 4.25}{\rightleftharpoons} A\cdot^- + H^+ \quad (10)$$

A breakdown of the total number of ascorbic acid radicals into per cent fractions (α) of specific forms as a function of pH is given in Figure 9.

The pH dependence of the ascorbic acid radical second-order decay can be explained by the following mechanism.

$$AH_2\cdot^+ + AH_2\cdot^+ \xrightarrow{k_{11}} AH_2 + A + 2H^+ \quad (11)$$

$$AH_2\cdot^+ + AH\cdot \xrightarrow{k_{12}} AH_2 + A + H^+ \quad (12)$$

$$AH\cdot + AH\cdot \xrightarrow{k_{13}} AH_2 + A \quad (13)$$

$$AH\cdot + A\cdot^- + H_2O \xrightarrow{k_{14}} AH_2 + A + OH^- \quad (14)$$

$$A\cdot^- + A\cdot^- + 2H_2O \xrightarrow{k_{15}} AH_2 + A + 2OH^- \quad (15)$$

The overall rate below pH 4 is given by the equation

$$k_{obsd} = \frac{k_{11} + k_{12}(K_1/[H]^+) + k_{13}(K_1/[H]^+)^2}{[1 + (K_1/[H]^+)]^2} \quad (II)$$

which was used to compute the theoretical curve (solid line) in Figure 6. Above pH 4 the rate constants k_{11}, k_{12}, and k_{13} are replaced by k_{13}, k_{14}, and k_{15} and equilibrium constant K_1 is replaced by K_2. The best values of the rate and equilibrium constants are given in Table V.

Table V. Rate and Equilibrium Constants for the Ascorbic Acid Free Radical at 23.5°

k_{11}	$(4.45 \pm 0.15) \times 10^8$ M^{-1} sec^{-1}
k_{12}	$(6.78 \pm 0.69) \times 10^8$ M^{-1} sec^{-1}
k_{13}	$(7.40 \pm 0.16) \times 10^7$ M^{-1} sec^{-1}
k_{14}	$(2.38 \pm 0.26) \times 10^8$ M^{-1} sec^{-1}
k_{15}	$(7.00 \pm 0.62) \times 10^4$ M^{-1} sec^{-1}
K_1	7.95×10^{-2}
K_2	5.63×10^{-5}

Supporting evidence for this mechanism was obtained from studies of ionic strength effects. While reactions 11 and 15 predict an increase in decay rate with increasing ionic strength for the first and third plateau regions (Figure 6), no effect is expected in the second plateau region representing reaction 13. These effects were confirmed by plotting the logarithm of the ratio of decay rate constants in the presence (k) and absence of salt (k_0) against ionic strength (Figure 8). At pH 3.3 the slope is zero, while at pH 9.8 it is unity. No systematic studies were carried out in the first plateau region, as the ionic strength was already too high for correct interpretations. When the ionic strength at pH 0.8 was increased by addition of sodium perchlorate, an increased decay rate was observed, indicating at least qualitatively that charged species are involved in reaction 11.

The increased rate of decay for ascorbic acid radicals (Figure 7) observed in the presence of ascorbate or phosphate is difficult to explain. The effect is most pronounced in the pH range 5 to 8.5, where reaction 14 is rate controlling. The dependence of k_{obsd} upon ascorbate or phosphate concentration is not linear. Since in

these experiments the total number of radicals generated (4 μM) was too small to affect the buffering capacity of the phosphate solutions, no pH shift occurred which could explain the change in k_{obsd}. The effect was also checked at pH 6.91 in the absence of buffers (see the Results section and Table II).

In view of these observations we assume for the present that complex reactions are involved despite the fact that the observed decay follows strictly second-order kinetics.

Acknowledgments. The authors wish to thank Drs. H. A. Schwarz, A. O. Allen, and J. M. Gebicki for their constructive criticism and many helpful suggestions. Thanks are also due to Mr. D. Sacker of the Medical Department for his kind help in the development of X-ray plates.

Crystal Structure of Nickel(II) Deoxophylloerythrin Methyl Ester 1,2-Dichloroethane Solvate. A Carbocyclic Porphyrin

Roger C. Pettersen*

Contribution from the Mellon Institute of Carnegie-Mellon University, Pittsburgh, Pennsylvania 15213. *Received October 29, 1970*

Abstract: The crystal and molecular structure of nickel(II) deoxophylloerythrin methyl ester 1,2-dichloroethane solvate, $C_{34}H_{36}N_4O_2Ni \cdot {}^1/_2C_2H_4Cl_2$, has been determined by three-dimensional X-ray techniques. Pertinent crystal data are: space group $P\bar{1}$, $a = 10.376$, $b = 11.749$, $c = 13.512$ Å, $\alpha = 90.70$, $\beta = 94.38$, $\gamma = 107.91°$, $Z = 2$. The structure was determined by conventional Fourier techniques and refined by full-matrix least squares. The weighted R factor for 4295 reflections is 5.8% and the unweighted R factor is 11.2%. The porphyrin molecule is nearly planar, with a very slight ruffling effect. No local deviations from planarity were observed except for the atoms of the carbocyclic ring E. The nickel atom was found to lie in the plane of the molecule. As determined for the structure of vanadyl deoxophylloerythroetioporphyrin, it was again noted that the distance between the metal atom and the nitrogen of ring C is shorter (1.89 Å) than the other three metal–nitrogen distances (av = 1.97 Å). This shortening is probably due to the added strain introduced by the fifth carbocyclic ring E.

Geochemists and chemists have been investigating the relationship between chlorophyll and the petroporphyrins since 1934 when Treibs isolated and identified etioporphyrin(III) (Etio) and deoxophylloerythroetioporphyrin (DPEP) from various samples of natural bituminous materials including oil, shale, and coal.[1] Treibs proposed a scheme whereby, in geological time, hemin could be degraded to Etio and chlorophylls a and b to DPEP. Much work has been done since Treibs' proposal, and although the situation has been shown to be much more complex than he originally supposed, his ideas appear to be largely substantiated. An excellent introduction and review of this interesting area of geochemistry appears in a recently published book.[2]

As a further contribution to this area of chlorophyll–porphyrin chemistry, a series of X-ray analyses was undertaken at Mellon Institute designed to provide quantitative structural information on porphyrin and chlorin compounds which have conformational features in common with chlorophyll a. The structure of vanadyl–DPEP (VO–DPEP) was the first to be determined in this series.[3] Nickel(II) deoxophylloerythrin methyl ester (Ni–DPE), the second and current structure, is quite similar to VO–DPEP, but the methyl propionate side chain places it a step closer to the chlorophyll a molecule.

Experimental Section

Ni–DPE was prepared and isolated by E. W. Baker of this laboratory. The starting material was pheophytin a, which was degraded to deoxophylloerythrin methyl ester.[4] The two central hydrogen atoms were replaced by a nickel atom by refluxing the ester with nickel acetate in a 1:1 mixture of glacial acetic acid and dimethylformamide. Crystals were grown by a vapor-phase diffusion of methanol into a 1,2-dichloroethane solution of Ni–DPE at room temperature. The unit cell dimensions were determined from a least-squares refinement of accurately measured values of 2θ for 30 high-angle reflections. The presence of 0.5 mol of 1,2-dichloroethane was indicated by a density measurement and later confirmed by the solution of the structure. The density was determined by flotation in aqueous potassium iodide solution. Table I lists the pertinent crystallographic data.

Intensity measurements were made on an automated General Electric XRD-5 spectrogoniometer equipped with a NaI scintillation counter and pulse-height discriminator. The radiation employed was nickel-filtered copper and the takeoff angle from the X-ray tube was set at 0.04°. The θ–2θ scan technique of Alexander and Smith was employed, using a variable scan range determined by the formula $2\theta_{scan} = 1.80 + 0.86 \tan \theta$.[5] The scan rate was 2.0°/min. The reflection settings were generated by the program DIFSET of the X-ray 67 system.[6] All of the generated reflections were stored on a magnetic tape and pulled off in groups of about 350 each using a program DATAPE written by R. F. Stewart. The output from this program took the form of a punched paper tape containing all necessary instructions to drive the Datex control unit of the diffractometer. Backgrounds were counted for 10 sec at both the high- and low-angle extremes of the scan range. An entire

* Address correspondence to the University Chemical Laboratory, Cambridge University, Cambridge, England CB2 1EW.

(1) A. Treibs, *Angew. Chem.*, **49**, 682 (1936).

(2) E. W. Baker in "Organic Geochemistry," G. Eglinton and N. T. J. Murphy, Ed., Springer-Verlag, Berlin, 1969, pp 464–497.

(3) R. C. Pettersen, *Acta Crystallogr., Sect. B*, **25**, 2527 (1969).

(4) E. W. Baker, A. H. Corwin, E. Klesper, and P. E. Wei, *J. Org. Chem.*, **33**, 3144 (1968).

(5) L. E. Alexander and G. S. Smith, *Acta Crystallogr.*, **15**, 983 (1962).

(6) J. M. Stewart, *et al.*, "X-Ray 67. Program System for X-ray Crystallography," Technical Report No. 67-58, 1967, Computer Science Center, University of Maryland, College Park, Md.